Mutual Coupling and Sensitivity Investigations of SIW-Based Antipodal Linear Tapered Slot Antennas in1-D and 2-D Array Configurations

Farzaneh Taringou[1,2], Thomas Weiland[1], Jens Bornemann[2]
[1] Technische Universität Darmstadt, Institüt fuer Theorie Elektromagnetischer Felder, Schloßgartenstr. 8, 64285 Darmstadt, Germany
[2] Department of Electrical and Computer Engineering, University of Victoria, Victoria, BC, V8W 3P6, Canada

***Abstract*—A comprehensive study of the impacts of mutual coupling in computationally expensive antenna arrays is presented. Single- and dual-polarized antipodal linear tapered slot antennas (ALTSAs), which are fed by coplanar waveguides (CPWs) and substrate integrated waveguides (SIWs), are arranged in 1-D and 2-D array configurations, operating between 21 GHz and 31 GHz. The influence of mutual coupling and element spacing sensitivity on radiation properties as well as return loss performances in 1-D and 2-D arrays are presented and discussed. The broadband performance of the individual array antenna element on low-permittivity substrate is verified by measurements.**

Index Terms—tapered slot antenna; antenna array; mutual coupling; substrate integrated waveguide

I. Introduction

The main advantages of the printed tapered slot antenna (TSA) [1, 2] are end-fire and nearly symmetric pattern characteristics, broad bandwidth and ease of fabrication as has been demonstrated up to millimeter-wave [3] and even terahertz frequencies [4]. It is primarily used in phased and scanning arrays [5, 6] as well as dual-polarized focal-plane imaging systems, e.g. [7].

Inter-element coupling and sensitivities in large antenna arrays can only be tackled by employing rigorous numerical techniques which is a computationally expensive task. For the simplicity of analysis, coupling effects are occasionally neglected. However, they are indispensable design parameters in feed systems with critical specifications and comparably high manufacturing costs.

Recently, different aspects, including mutual coupling, of several printed-circuit Vivaldi arrays have been investigated for focal-plane array applications [7] – [11]. All such systems operate in the lower Gigahertz frequency range and use microstrip-to-slotline transitions to feed individual Vivaldi elements. As frequency increases, however, and especially with a view to millimeter-wave applications [12], coplanar waveguide (CPW) feeds are known to be more suitable due to their advantages over microstrips with respect to surface-mount integration, lower phase velocity variation, lower cross talk and radiation, e.g. [13]. Since a direct connection between a CPW and a TSA requires bond wires or air bridges [14], which add complexity to the fabrication of an array, a transition from CPW to substrate integrated waveguide (SIW) [15] to TSA is

(a)

(b)

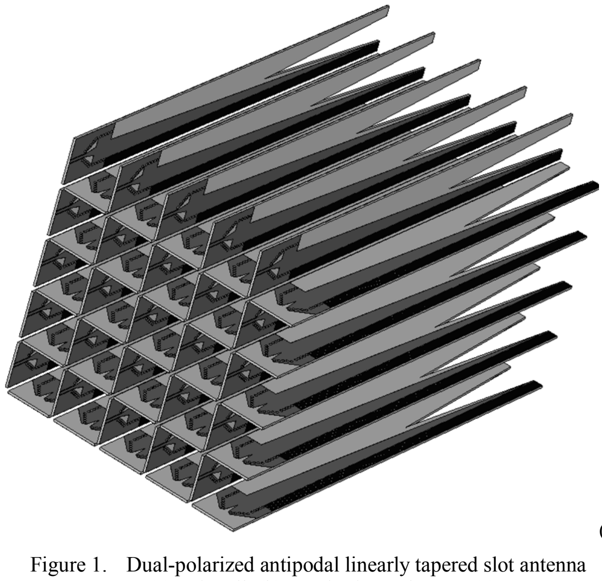

(c)

Figure 1. Dual-polarized antipodal linearly tapered slot antenna arrangements: (a) unit cell, (b) 1-D horizontal array, (c) 2-D array.

more appropriate. Due to the waveguide-like field pattern in the SIW, the two fins of the TSA are located on opposite sides of the substrate, thus making it an antipodal linearly tapered slot antenna (ALTSA).

In order to assess the performance of CPW-fed SIW-based ALTSAs, this paper investigates the impact of mutual coupling in single- and dual-polarized 1-D and 2-D arrays (c.f. Fig. 1) for broadband 21 GHz to 31 GHz operation.

II. ARRAY DESIGN

The dual-polarized unit cell of the CPW-SIW-fed ALTSA is depicted in Fig. 1a with the vertical part showing the top and the horizontal part the bottom metallization of a single antenna element. Their 1-D and 2-D extensions are shown in Fig. 1b and Fig. 1c, respectively.

Fig. 2 displays the front view of the individual array element. For the feeding structure, a CPW-to-SIW transition [16] is employed. The selected substrate is RT/Duroid 6002 with ε_r=2.94, tanδ=0.0012, substrate thickness h=0.508mm, metallization thickness t=17.5 µm, and conductivity σ=5.8x10^7 S/m. The fins are corrugated [17], and the substrate is removed close to the aperture to satisfy conditions stipulated in [2]. The height of the element is 10.2 mm.

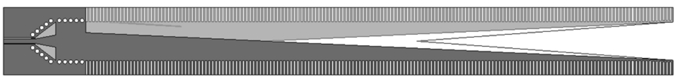

Figure 2. Front side of individual ALTSA array element with CPW-to-SIW transition, corrugations and removed substrate close to aperture .

The array geometry in this study follows the very basic configuration of an equally spaced linear array with five and 25 elements as shown in Fig. 1b and Fig. 1c, respectively. The centre-to-centre element spacing is one wavelength, λ_0 =11.5 mm, at the midband frequency of 26 GHz. The elements are excited with equal amplitude and phase.

In order to identify individual elements in the next section, Fig. 3 shows polarization and element numbering of the 2-D ALTSA array in Fig. 1c. The black and red squares represent the central elements identified in Fig. 4 for horizontal and vertical polarizations, respectively. For a 1-D array according to Fig. 1b, only the lowest row in Fig. 3 is used. The bottom left element in Fig. 3 represents the unit cell of Fig. 1a.

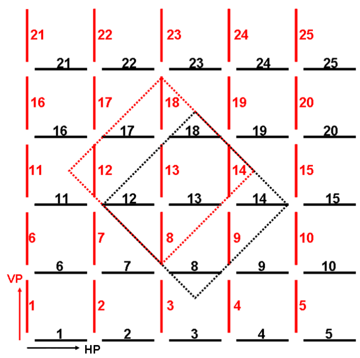

Figure 3. Polarization and element numbering of the 2-D ALTSA array of Fig. 1c.

III. RESULTS

This section presents the results of different ALTSA array scenarios. Unless otherwise stated, all simulations are performed within the time-domain solver of CST Microwave Studio.

With respect to the input reflection coefficients, Fig. 4 shows performance comparisons between the unit-cell ALTSA (Fig. 1a), the 1-D array of Fig. 1b and the 2-D array of Fig. 1c. In Fig. 4a, the influence of mutual coupling is minimal as the only other element present is positioned at a 90-degree angle (Fig. 1a). It is demonstrated that the input return losses of both polarizations of the unit cell are better than 19 dB between 21 GHz and 31 GHz. Note that the respective unit-cell reflection coefficients are replotted in Fig. 4b to Fig. 4e for comparison.

Fig. 4b and Fig. 4c show individual input reflection coefficients of the 1-D array of Fig. 1b in horizontal (HP) and vertical (VP) polarizations, respectively. Of course, deteriorations of the return losses are observed compared to those of the unit cell, but they are within reasonable limits. The return losses are still better than 16.5 dB and 17.5 dB, respectively, between 21 GHz and 31 GHz, thus down by a maximum of 2.5 dB from the original 19 dB.

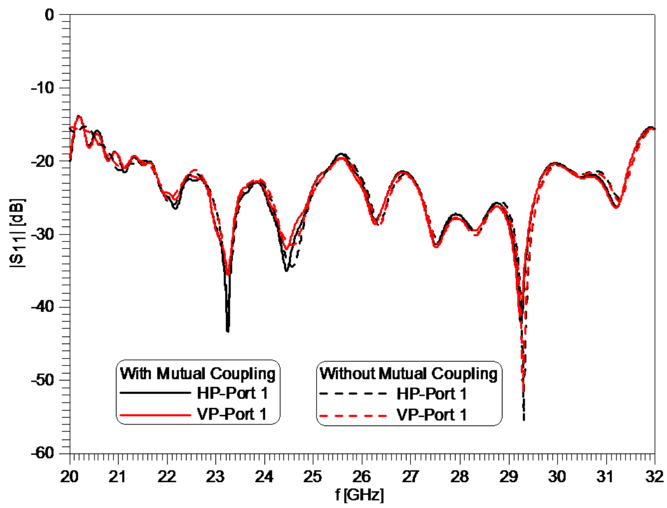

(a)

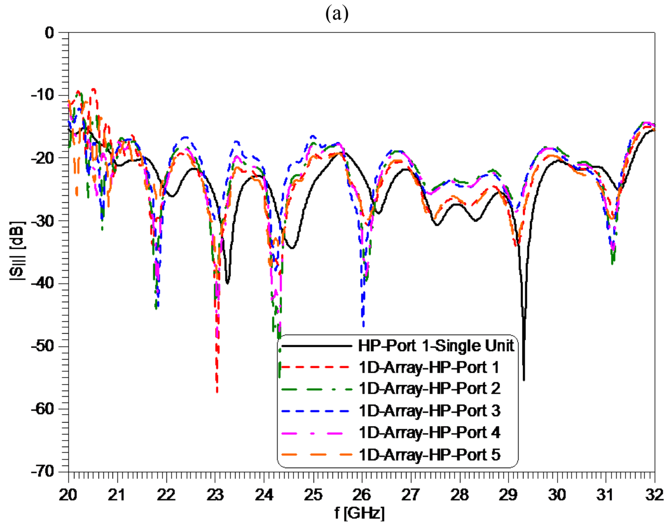

(b)

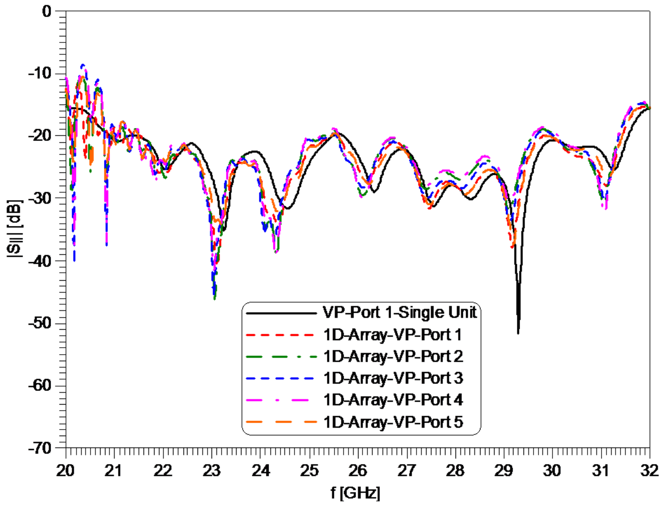

(c)

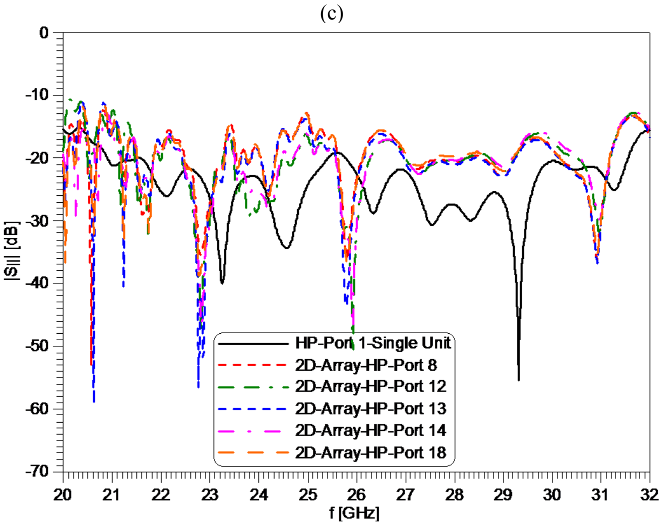

(d)

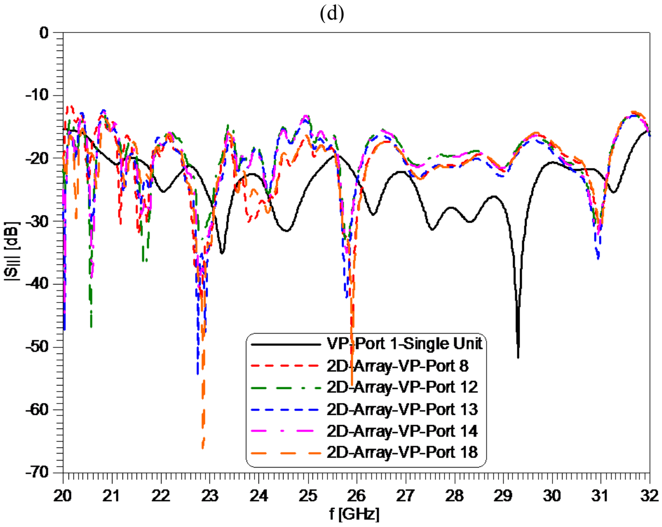

(e)

Figure 4. Performance comparison of the input reflection coefficients of different arrays: (a) the ALTSA unit cell (Fig. 1a); (b) 1-D array (Fig. 1b), horizontal polarization; (c) 1-D array (Fig. 1b), vertical polarization; (d) 2-D array (Fig. 1c), horizontal polarization; (e) 2-D array (Fig. 1c), vertical polarization.

A higher deterioration of the return loss is observed for the 2-D array in Fig. 4d (horizontal polarization) and Fig. 4e (vertical polarization) and represents the unmistakable impact of the inter-element coupling. The worst input return losses between 21 GHz and 31 GHz seen into ports 8, 12, 13, 14 and 18 of the respective polarizations (c.f. Fig. 3) are at 12.5 dB (HP, Fig. 4d) and 13 dB (VP, Fig. 4e) . Although these values are up to 6.5 dB down from the unit-cell design, they are still well above the commonly accepted value of 10 dB (VSWR≈2).

The principle-plane radiation patterns of the dual-polarized 1-D horizontal array of Fig. 1b as well as the 2-D array of Fig. 1c are respectively shown in Fig. 5a and Fig. 5b at 24 GHz. As expected, the respective beam widths in horizontal (HP) and vertical (VP) polarizations are very similar. The influence of mutual coupling on the patterns is obvious, especially with respect to side-lobe levels. However, these effects are less pronounced compared with those in the return loss investigation.

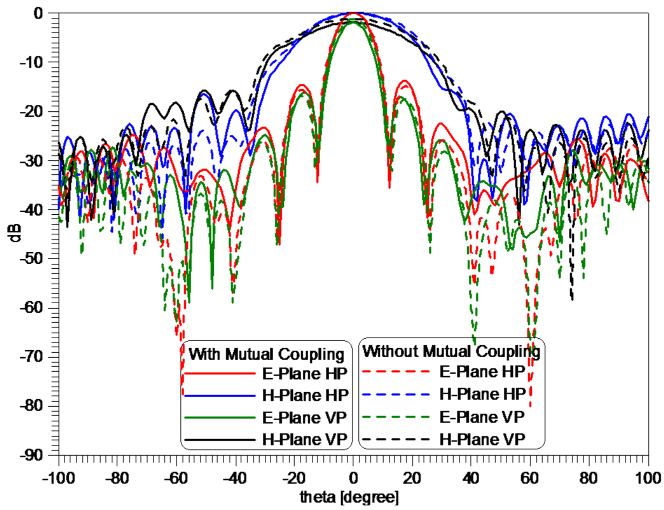

(a)

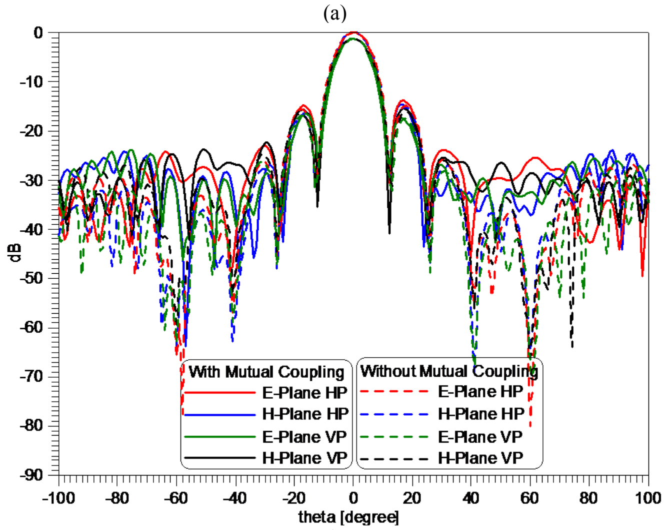

(b)

Figure 5. Principle-plane radiation patterns of dual-polarized arrays: (a) 1-D ALTSA array (Fig. 1b); (b), 2-D ALTSA array (Fig. 1c).

In the model used for Fig. 5, the cross-polarization performance cannot be assessed when all ports are simultaneously and uniformly excited. Therefore, Fig. 6 shows results for a single-polarized 1-D array with both co- (HP) and cross-polarized (VP) patterns. It is observed that the principle-plane cross-polarization levels degrade by 2 dB and that the co-polarized E-plane and H-plane beams are slightly narrowed. Note that only the main-plane cross-polarizations are plotted. As is shown in [12] for a single array element, 45-degree cross-polarization values are approximately 1 dB higher than those in the main planes.

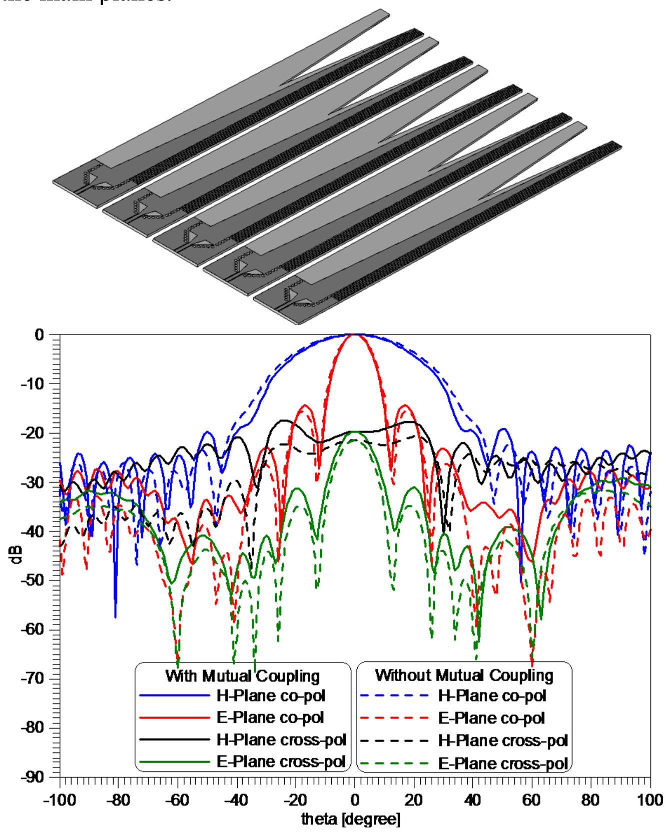

Figure 6. Co- and cross-polar radiation patterns of the single-polarized array 1-D array with main horizontal polarization.

All array parameters are subject to sensitivities with respect to fabrication, temperature and other factors. Under normal circumstances and in a stable environment, temperature changes are of low concern, and tolerances of the individual array elements are controlled by printed-circuit board technologies. The next sensitive parameter in the assembly of the array is the element spacing.

Therefore, Fig. 7 shows return loss (Fig. 7a) and pattern investigations (Fig. 7b) of the single-polarized 1-D array of Fig. 6. Note that the nominal value is 11.5 mm and that the element width 10.2 mm. The variation of the return loss of the central element is more pronounced in the higher frequency range as the changes with respect to wavelength are larger. However, between 21 GHz and 31 GHz, the return loss stays below 14.5 dB. The H-plane beam change in Fig. 7b is only minor, and element spacing affects the side-lobe levels and the main beam only below -10 dB. In the narrower E-plane, however, a more significant impact of the element spacing is expected.

This is shown in the E-plane pattern of the 2-D array in Fig. 8, where the pattern is clearly more sensitive to element spacing. The half-power beamwidth reduces with increasing element spacing; the side lobes increase by about 1.5 dB and move closer to the main beam.

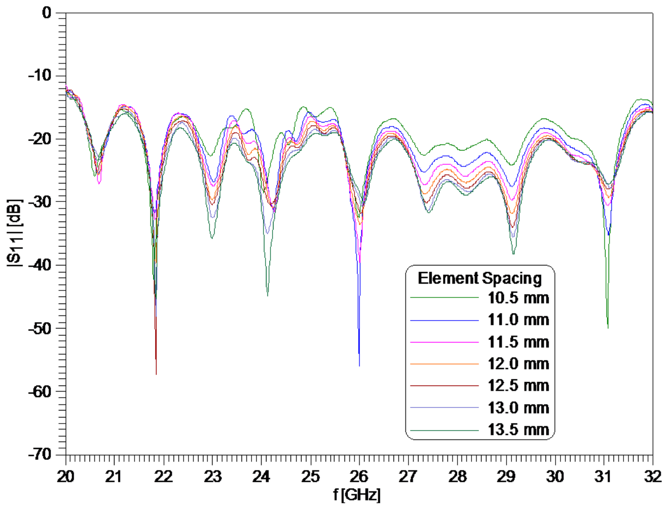

(a)

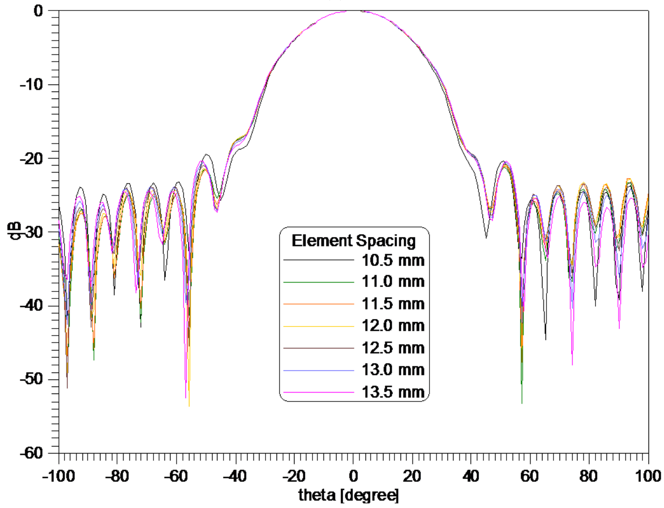

(b)

Figure 7. Sensitivity analysis with respect to element spacing of the array in Fig. 6; (a) return loss, (b) H-plane pattern.

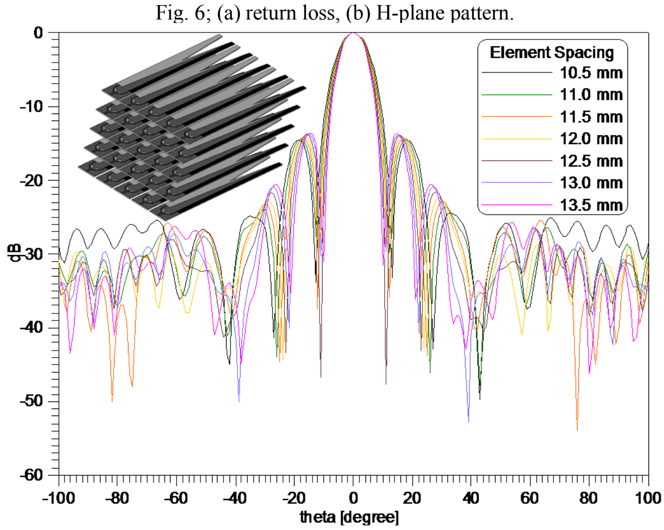

Figure 8. Sensitivity analysis with respect to element spacing of the main beam pattern of a single-polarized 2-D array.

In order to relate the above investigation to practical values, a single element of the antenna presented in Section II has been prototyped and measured. Fig. 9 shows a comparison between measurements and two software packages, the time-domain solver of CST, which is used throughout this investigation, and the frequency-domain finite-element solver HFSS. It is demonstrated that the agreement between simulation and experimental results is reasonable. The worst return loss levels between 21 GHz and 31 GHz are predicted as 18.8 dB (CST) and 19.2 dB (HFSS). The respective measured value is 15.8 dB.

The two simulated gains agree extremely well; however, the measured performance is slightly below those of the simulations above 26.5 GHz, where a different standard gain horn (Ka-band) has been used. Between 21 GHz and 26 GHz, some inconsistencies in the boresight E-plane measurements produce the wavy response in the gain measurements. In general, though, the agreement is good and provides credibility to the previous investigation on mutual coupling and element-spacing sensitivity.

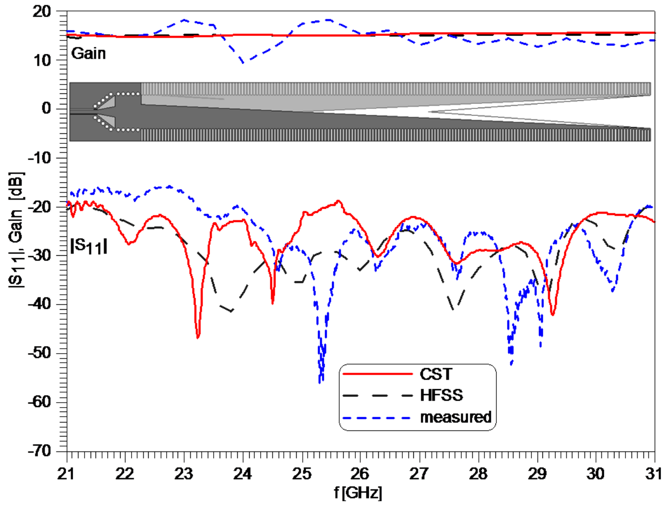

Figure 9. Comparison between simulations (CST and HFSS) and measurements for input reflection coefficient and gain in dB of the 21-31 GHz ALTSA prototype.

IV. CONCLUSIONS

Inter-element coupling in antenna arrays is an inevitable but computationally expensive factor. The performances of dual-polarized 1-D and 2-D ALTSA array configurations are presented in terms of return loss and radiation patterns - with and without taking into account mutual coupling. Compared to previous work, the single element antenna is fed by a combination of CPW and SIW technology to achieve broadband operation over the 21 GHz to 31 GHz frequency range. Compared to a single element, the input return loss of a 1-D array exhibits a degradation of 2.5 dB. Main-plane cross-polar levels in a single-polarized array increase by 2 dB due to mutual coupling. An additional dB is expected in the diagonal planes. The sensitivity of the performances of single-polarized 1-D and 2-D arrays with respect to element spacing show return loss increases by 2 dB, and side-lobe level and beam width changes, especially in the narrow pattern of the array.

Measurements of a single-element prototype are presented. Experimental and simulated gain and return loss results are in reasonable agreement and validate the computationally expensive investigations on single- and dual-polarized 1-D and 2-D ALTSA arrays.

REFERENCES

[1] P. J. Gibson, "The Vivaldi aerial," Proc. 9th European Microwave Conf., pp. 101-105, Brighton, U.K., June 1979.

[2] K.S Yngvesson, D.H. Schaubert, T.L. Korzeniowski, E.L. Kollberg, T. Thungren, and J. F. Johansson "Endfire tapered slot antennas on dielectric substrates," *IEEE Trans. Antennas Propagat.*, vol. 33, pp. 1392-1400, Dec. 1985.

[3] J. B. Rizk and G.M. Rebeiz, "Millimeter-wave Fermi tapered slot antennas on micromachined silicon substrates," *IEEE Trans. Antennas Propagat.*, vol. 50, pp. 379-383, Mar. 2002.

[4] H.J. Tang W. Hong; G.Q. Yang, and J.X. Chen, "Silicon based THz antenna and filter with MEMS process," Proc. Int. Workshop Antenna Technology (iWAT), pp. 148-151, Hong Kong, Mar. 2011.

[5] K.S. Yngvesson, T.L. Korzeniowski, Y.S. Kim, E.L. Kollberg, J.F. Johansson, "The tapered slot antenna – A new integrated element for millimeter wave applications," IEEE Trans. Microwave Theory Tech., vol. 37, pp 365-374, Feb. 1989.

[6] H. Holter, T.-H. Chio, and D.H. Schaubert, "Experimental results of 144-element dual-polarized endfire tapered-slot phased arrays," IEEE Trans. Antennas Propagat., vol. 48, pp 1707-1718, Nov. 2000.

[7] B. Veidt, G.J. Hovey, T.Burgess, R.J. Smegal, R. Messing, A.G. Willis, A.D. Gray, and P.E. Dewdney, "Demonstration of a dual-polarized phased-array feed," *IEEE Trans. Antennas Propagat.*, vol. 59, pp. 2047-2057, June 2011.

[8] D. Gonzalez-Ovejero, F. Mesa, C. Craeye, and R.R. Boix, "Efficient analysis of mutual coupling in periodic and non-periodic printed antenna arrays," Proc. European Conf. Antennas Propagat., pp. 220-223, Prague, Czech Republic, Mar. 2012.

[9] E. de Lera Acedo, E. García, V. González-Posadas, J.L. Vázquez-Roy, R. Maaskant, and D. Segovia, "Study and design of a differentially-fed tapered slot antenna array," *IEEE Trans. Antennas Propagat.*, vol. 58, pp. 68-78, Jan. 2010.

[10] M.V. Ivashina, O. Iupikov, R. Maaskant, W.A. van Cappellen, and T. Oosterloo, "An optimal beamforming strategy for wide-field surveys with phased-array-fed reflector antennas," *IEEE Trans. Antennas Propagat.*, vol. 59, pp. 1864-1875, June 2011.

[11] P. Benthem, G.W. Kant, S.J. Wijnholds, M.J. Arts, R. Maaskant, M. Ruiter, and E. van der Wal, "Aperture array development for future large radio telescopes," Proc. European Conf. Antennas Propagat., pp. 2601-2605, Rome, Italy, Apr. 2011.

[12] F. Taringou, D. Dousset, J. Bornemann and K. Wu, "Broadband CPW feed for millimeter-wave SIW-based antipodal linearly tapered slot antennas," IEEE Trans. Antennas Propagat., Vol. 61, Apr. 2013, in press.

[13] I. Wolff, "Design rules and realisation of coplanar circuits for communication applications," Proc. European Microwave Conf., pp. 36-41, Madrid, Spain, Sep. 1993.

[14] W. Grammer and K.S. Yngvesson, "Coplanar waveguide transitions to slotline: Design and microprobe characterization," IEEE Trans. Microwave Theory Tech., vol. 41, pp. 1653-1658, Sep. 1993.

[15] Y. Cassivi, L. Perregrini, P. Arcioni, M. Bressan, K. Wu, and G. Conciauro, "Dispersion characteristics of substrate integrated rectangular waveguide," IEEE Microwave Wireless Comp. Lett., vol 12, pp. 333-335, Sep. 2002.

[16] F. Taringou, D. Dousset, J. Bornemann and K. Wu, "Substrate-integrated waveguide transitions to planar transmission-line technologies", IEEE MTT-S Int. Microwave Symp. Dig., pp. 1-3, Montreal, Canada, June 2012.

[17] H. Sato, Y. Takagi, and K. Sawaya, "High gain antipodal Fermi antenna with low cross polarization," IEICE Trans. Commun., vol. E94-B, pp. 2292-2297, Aug. 2011.